Final response to review

Dear Editor,

We are grateful to both reviewers in contributing constructive suggestions and pointing out missing information in order to improve the manuscript. Please, find below a point-by-point reply (mainly along the lines that already were published online) on the points raised by both reviewers. The accordingly revised version with changes produced by *LaTeXDiff* is attached below these replies.

In particular, let us point out that we had a long discussion on the possibility of including analytic solutions raised by Reviewer 1 to the benchmark presented in the article. This discussion and investigation resulted in our conclusion that analytic solutions only would exist for an oversimplified setup that – in our view – does not test the basic concept of multi-layered solid Earth deformation with the main aspect of replacing Winkler foundations by including the pre-stress advection in the weak formulation as presented here.

In the name of all co-authors with kind regards,

(Thomas Zwinger)

Response to reviewer 1 (PingPing Huang)

The module proposed in this article is a good alternative in modeling Glacial Isostatic Adjustment (GIA) because it takes advantage of an open-source and free FEM package Elmer. The article is well written with a clear structure. I can support publishing the article if the author can provide more details of the method and more benchmark tests:

We thank for the generally positive assessment of the reviewer and are grateful for the work invested to improve the manuscript. Please, find our response inline to the suggestions:

In section 2, what are the boundary conditions on internal boundaries and external surface for a flat Earth model and how are they implemented in the model ?

The main new aspect introduced in this paper is, that we are solving the complete set of equation over the whole domain and hence do not need to prescribe Winkler foundations. Accounting for layer discontinuities in material parameters is being taken care by the fact that the term – in contrary to the modification of commercial codes, where this only occurs in the body force – is appearing in the system matrix and produces the restoring force as a natural condition. We will expand the current explanation in the text:

> *This means that we are able to impose discontinuities in parameters over elements anywhere in the discretized computing domain without placing Winkler foundation boundaries at layer interfaces. By including this term in the weak formulation of the problem, the method then automatically applies the needed restoring force on element boundaries with jumps in material properties or gravity, without the need to place boundaries in the mesh.*

by another sentence:

> *This means that we are able to impose discontinuities in parameters over elements anywhere in the discretized computing domain without placing Winkler foundation boundaries at layer interfaces. In other words, no boundary conditions have to be set at internal layer boundaries. By including this term in the weak formulation of the problem, the method then automatically applies the needed restoring force on element boundaries with jumps in material properties or gravity, without the need to place boundaries in the mesh.*

For the external boundaries we will add the following paragraph at the end of section 3.3:

We apply zero deformation at the side and the bottom boundaries. At the upper surface, we impose the load as described in the paragraph above.

In terms of solving Equation (9), what are the detailed form of the test and weighting functions and what is the integration method ?

Indeed, this information was missing. We will add the following paragraph after equation (9):

Equation (9) is solved using the standard Galerkin method with – in the case of the benchmark described in section 3 - first order basis functions. Apart from this particular choice, Elmer provides a variety of possible basis functions left to the choice of the user. The iteration for the viscous contribution is computed on the Gaussian integration points. In case of incompressibility, stabilization has to be applied by the residual free bubble method.

In section 3. when doing benchmark tests, it is more convincing that if the numerical solution can be compared with the analytical or semi-analytical solution. Therefore, it is good to compare the result from Elmer/Earth with that from normal-mode method for a Heaviside single harmonic load and a flat Earth model.

We came to the conclusion that the multi-layered model we are presenting does not have an analytic solution to compare to. We are aware that there are existing analytic solutions for strongly simplified two-layer configurations with continuous density distribution (e.g., Appendix A in England et al., 2013). Nevertheless, our model contains several layers with different densities and varying gravity . Since this variation of materials in the mantle is an inherent feature of our model, we conclude that we are not able to compare to an analytical solution.

Below are some small issues:

Figure 1 and Figure 2: font size on axises is too small.

We will provide figures with a larger font

Line 148: why does a high viscosity (e.g. 1 x10^{44} Pas) in Lithosphere enables an approximately elastic behaviour?

At the centennial timescale of our benchmark, the extreme value of the viscosity ensures that all loads are accommodated by an elastic response of the Lithosphere. Theoretically, this can be explained by an extreme resulting high value of the Maxwell-time (viscous relaxation time) of 10^{33} seconds (10^{23} years). We will insert the following sentence:

This can be justified by the Maxwell-time $t_m = \nu/\mu$ being of the order of 10^{33} seconds (10^{23} years), which indicates that viscous effects only would be significant at timescales several order of magnitudes larger than the timing of the load signal in our experiment or even on timescales of glacial cycles on Earth.

Why the viscosity of upper and lower mantle are set to be 1 x10^{18} Pas and 1 x10^{22} Pas respectively ?

The latter value is a commonly used value for the mantle, the relatively low value of 1 x10^{18} Pa s for the upper mantle mainly is motivated to accelerate the computation.

References

P. C. England, R. T. Walker, B. Fu, M. A. Floyd, A bound on the viscosity of the Tibetan crust from the horizontality of palaeolake shorelines,
Earth and Planetary Science Letters, Volume 375, 2013, pp 44-56, https://doi.org/10.1016/j.epsl.2013.05.001.

Response to reviewer 2 (Surendra Adhikari)

This paper presents a new module implemented in Elmer, termed Elmer/Earth, that allows users to compute the solid Earth's deformational response to the applied surface loads. Given the observation of rapid response of solid Earth to ongoing ice mass loss and its possible stabilizing feedback to ice sheet dynamics (e.g., Barletta et al.,2018, doi: 10.1126/science.aao1447), Elmer/Earth is a welcome addition to Elmer particularly in light of Elmer/Ice (Gagliardini et al., 2013, doi: 10.5194/gmd-6-1299-2013) that can simulate evolving ice load subject to atmospheric and oceanic forcings.

We thank for the generally positive assessment of the reviewer and are grateful for the detailed work invested to improve the manuscript. Please, find our response inline to the suggestions:

For the reasons that follow, however, I am not so sure about the utility of this new module to fulfill the purpose of improving our understanding of ice-sheet/solid-Earth interaction. Change in ice mass directly loads the underlying solid Earth, and hence, induces its deformation. Ice mass change also modulates the ocean mass, satisfying mass conservation in the Earth System. The change in ocean load contributes to the solid Earth deformation. Ignoring ocean load may underestimate the magnitude of modelled displacement field by about 10%, at least around the ice-bedrock-ocean interfaces. Elmer/Earth clearly lacks the ability to capture mass conserving ocean load induced by ice mass change, limiting its utility for the rigorous analysis of ice-sheet/solid-Earth interaction. Furthermore, both the ice and ocean mass change deform the geoid field, which further amplifies the strength of stabilizing feedbacks of the solid Earth to marine ice sheet dynamics. This element is also overlooked in the current version of Elmer/Earth. At a minimum the authors should acknowledge this limitation, with reference to recent works on the topic of ice-sheet/solid-Earth/sea-level interaction (e.g., Adhikari et al., 2020, doi: 10.5194/tc-2020-23). Elmer/Earth perhaps is more suitable for predicting local- or regional-scale hydrology (including ice) induced displacement fields.

That is a correct statement. We have clarified that we recommend the model's application only in a regional context by adding the following sentence in the conclusions:

> *Elmer/Earth for the time being is a so-called flat-earth model (Wu, 2004). In its current state it ignores sphericity and self-gravitational effects as well as neglects to account for the deformation induced by redistribution of ocean water masses. Consequently, future applications of this particular model version should be confined to regional studies of ice-sheets or highly localized loads, such as glaciers and ice-caps.*

For the suggested reference (Adhikari et al., 2020), we would like to point out that this is a paper that currently is in review and was not available for citation at the time this manuscript was submitted.

I find that the lateral boundary conditions imposed in Elmer/Earth may be problematic for its application to continental-scale ice sheet. They have simply considered a "large enough" horizontal extent of the domain and set displacement vector to zero at the lateral boundaries. For Antarctic Ice Sheet, for example, one may require horizontal extent of the domain to be on the order of tens of thousands of kilometers. In such situations, the effects of Earth's sphericity are not certainly negligible unlike in the testcase considered in the paper (line 135). Either a justification about this inconsistency or an acknowledgement of this limitation is required.

We will mention the neglected sphericity and its limitations in the text presented in the conclusions (see above) and also drop a note on this limitation in the new text describing the implementation of boundary conditions (see further below and response to comment on line 137/138).

Providing a bit more elaborative description of Theory (Section 2) would be useful, especially for those who are not familiar with Wu (2004, doi: 10.1111/j.1365-246X.2004.02338.x). Section 2 of the Wu paper is very informative, and all I see in this paper is a list of equations (with minimal explanation) that are deduced from Wu paper for the case of incompressible viscoelastic Earth that lacks self-gravitation and sphericity. Also, missing in this section is the (mathematical) description of boundary conditions.

We already described the complete model as derived in Section 3 of Wu (2004). In order to make it easier for the reader to evaluate which simplification have been taken place, we will add the following paragraph to the existing presentation of (currently) equation (4) in Section 2:

> *The linearized elastic equation of motion for earth deformation (Wu, 2004) is given by*
>
> $$\nabla \cdot \boldsymbol{\tau} - \nabla(\rho_0 \boldsymbol{g}_0 \cdot \mathbf{d}) - \rho_1 \boldsymbol{g}_0 - \rho_0 \nabla \phi_1 = \mathbf{0} \quad (4)$$
>
> *Where ρ_0 and $\boldsymbol{g}_0$ are hydrostatic background density and gravity, respectively, and ρ_1 is the perturbed density. The direction of $\boldsymbol{g}_0$ is in negative radial direction. According to Wu (2004, section 3), a flat-earth model is derived from (4) by assuming incompressibility and ignoring self-gravitational effects (i.e., redistribution of mass), making the third and fourth term vanish. Further, sphericity is ignored, leading to changes aligned with the unit vector of a Cartesian system in vertical direction, $\boldsymbol{e}_z$. This leads to the equation of motion for a non-self-gravitating flat-earth model with layer-wise constant material. It reduces to a balance between the divergence of the stress (first term) and a restoring force due to the advection of pre-stress of the material (Wu, 2004)*
>
> $$\nabla \cdot \boldsymbol{\tau} - \rho g \nabla(\boldsymbol{e}_z \cdot \boldsymbol{d}) = \mathbf{0} \qquad (5)$$
>
> *Here, $\rho = \rho_0$ and $g = |\boldsymbol{g}_0|$ is the magnitude of the local acceleration by gravity. …*

For the boundary condition, we will add the following sentence directly after (currently) equation (9) in Section 2.1:

> *The system is completed by boundary conditions that are either provided by a value for any component of the stress-vector, $= \boldsymbol{\tau} \cdot \boldsymbol{n}$, in the second integral (Neumann condition) of equation (10 , former 9) or by imposing a value for any component of the deformation vector, $\mathbf{d}$ (Dirichlet condition).*

And we explicitly state the boundary conditions for the benchmark in Section 3:

> *At the free surface we apply the load of the disc for the first 100 years into the simulation. Thereafter, the natural boundary condition, namely a vanishing stress vector, applies to the whole surface. At all other boundaries we impose a zero-deformation condition, i.e., $\mathbf{d} = \mathbf{0}$.*

A few suggestions on the usage of terminologies: Visco-elastic => viscoelastic; Earth=> solid Earth; Finite Element => finite element. So, the title would be "…viscoelastic solid Earth module…"
We will change accordingly

There is something about the word "flat-earth" that does not look right to me (especially in the era of social media). I would consider avoiding it.
We are well aware of the distorted connotation of the term in some communities with a – let us say - weird alternative approach to Earth science. Yet, the term has a scientific significance as it is used in the main reference (Wu, 2004) and it would be difficult for the reader to make the connection therein. We have retained the standard use in model studies of 'flat earth'. We are sure that the readers of this journal will apply the correct interpretation of this word.

Line 25: Is this timescale required for a "complete" relaxation of mantle? Or e-folding relaxation?
This is referring to a typical "Maxwell" relaxation time, rather than a complete relaxation. It is intended to be merely an indication of the timescales one could expect to observe viscoelastic relaxation over due to changes in ice loading with the point that some regions experience a very quick response due to low viscosity underlying mantle. We do not feel it is necessary to include this in the text as it may be confusing for some readers. We have however quantified the more rapid timescale as follows:

> *…although typically thought to occur over several thousands of years (Whitehouse, 2018, and references therein), recent studies have shown some regions undergoing much more rapid (decadal) rebound in response to present-day changes (Nield et al., 2014; Barletta et al., 2018)….*

Around line 30: Evolving bedrock also modulates the gravitational driving stress of the ice sheet and hence its dynamics (see Figure 6 of Adhikari et al., 2014, doi:10.5194/se-5-569-2014)
We include this reference

Line 33: Provide references, e.g. Schoof (2007, doi: 10.1029/2006JF000664).
We will include this citation on line 33.

Line 41: Best performing => in terms of computational ability? Or, its ability to match, say, bedrock GPS data?
Both, but mainly in terms of numerical performance. The shortcomings on physics are mentioned in the sentence to follow. We will add:

> *Of these, Le Meur and Huybrechts (1996) found the best performing is the "ELRA" model (elastic lithosphere with relaxing asthenosphere) which is widely used in ice-sheet modelling, mainly due to its simplicity and fast computations.*

Line 41: widely used => Not sure about this(!). Provide references at least. Again, for the reason I noted in the beginning of this review, even if this method is "widely" used it certainty is not the most accurate one.
It is in our view an up until recently widely used method. We will add another reference (Greve, 2001) to the already existing references (Le Meur and Huybrechts, 1996; Rutt et al., 2009). In no way do we claim that its popularity compensates for its shortcomings, which we believe are sufficiently mentioned in the sentence that follows: *However, Bueler et al. (2007) found significant differences …*

Line 53: suggested rewording: "...a full Stokes ice sheet model capable of yielding high wave number loads that is essential to model high-res solid Earth rebound"
We reword accordingly

Line 56: high gradients => of what?
We reformulate:

> *Finite Elements have the advantage that they in general can use unstructured meshes in order to provide the needed resolution in regions where either physics or geometry demand it while keeping the model size limited.*

Line 65: Cauchy stress => Cauchy stress tensor
We will change the text according to this suggestion

Line 66 (and elsewhere): deformation vector => displacement
We will change the text according to this suggestion

Line 69: Suggested rewording: "...motion that conserves linear momentum for a non-gravitating...layered material..."
As shown above, we completely dropped the brackets.

Line 74: Why do you need to introduce d_z? Simply write "...vector product e_z . d"
We dropped this sentence.

Line 79: Given the limited description of Theory (as noted above), not sure I follow what you exactly mean by "avoids singularity...as Poisson ratio approaches". Either refer this statement to some equation or delete it altogether
We reformulate to:

> *… avoids the singularity of the first Lamé parameter* $\lambda = E\eta/((1+\eta)(1-2\eta))$ *in the limit of the Poisson ratio approaching* $\eta \rightarrow ½$ *(e.g., Greve and Blatter, 2009; p 41).*

Line 84: Why 10 layers? Be generic.
Added:

> *… of several layers due to the resolution of changing material parameters.*

Line 121: The model is fixed in all directions => What do you mean by fixed? Dirichlet conditions with zero displacement? Again, you need to talk about boundary conditions in Theory section.
We reformulate:

> *…and has zero deformation imposed on its lateral boundaries.*

Line 135: "sea-level equation" => Need to provide a qualitative description of what it means if it is relevant at all (else simply delete the sentence). Not all readers would get what it means
We delete this sentence.

Line 137/138: Looks like it is 40,000 km (see Figure 1); and that would be 800 times larger? Again, Is the sphericity effect negligible for such a large spatial scale?
No, 2×10^6 m make 2,000 km in each direction, which gives 4,000 km and not 40,000 km in total span. Following the request of reviewer 1, we will increase the resolution of the annotation in Fig. 1 in order to make it better readable.
The flat-earth approach, with the necessary large lateral extents, has been shown to be accurate when computing deformation for ice loads as large as the Laurentide ice sheet (Wu and Johnston, 1998).
Nevertheless, we are computing a benchmark here and – as should be implicitly clear by load's small size of only 50 km in radius - in no way claim that this resembles a continental ice-sheet. Placing the boundaries so far out simply avoids any influence of boundaries on the displacement close to the centre. That motivation is reflected by the already existing line (and reference therein): *This distance is 80 times the diameter of the test load which is more than sufficient to allow mantle deformation below the ice load (Steffen et al., 2006).*

Line 144: "has a resolution equivalent" => "has a spectral resolution equivalent"
We will change the text according to this suggestion

Figures 1/2: Combine these as Figure 1a and 1b?
We will evaluate whether it is possible to combine them and still introduce larger annotation (as requested by reviewer 1).

Line 152: zero time => t = 0
We will change the text according to this suggestion

New Figure (that corresponds to Figure 4): Would be useful to show a new figure with displacement vs. distance away from the load center for select times (including at t=0 to show the elastic displacement fields).
We will include such a figure.

Around line 175: Acknowledge that ABAQUS uses compressible Earth (see Table 1 caption). Elmer/Earth solves for incompressible Earth.
This was an error in the text. Whilst ABAQUS can implement some aspects of compressibility (e.g. with a Poisson's ration < 0.5) it cannot change the density of elements with time. We use a high Poisson ratio in the benchmarking case to simulate incompressibility. We therefore remove "compressible" from Table 1 caption.

Section 5.2: I was wondering whether you maintain the same mass for different experiments (by adjusting ice height). Otherwise the discrepancy in solutions maybe (at least partly) due to the fact that you are loading the solid Earth with slightly different loads (i.e., net mass) and not necessarily do to the coarseness or fineness of computational mesh.
We are not completely sure we understand this question. We assume that it is about whether we change the net mass of the ice-disc in order to compensate for a lower resolution in the centre of the domain. We do not think that this is the case, since we impose a load and the mesh resolution (i.e. what is being tested) is inherent in how the disc load is represented in the model.

Figure 6 caption: Vertical deformation => Vertical displacement
We will change the text according to this suggestion

Lines 241: For the reasons noted early on, I am afraid that the utility of Elmer/Earth to accurately capture solid Earth's feedback to ice sheet dynamics (within Elmer/Ice) is limited. At least, it should be acknowledged. I would highlight the utility of Elmer/Earth for general (regional/local) loading studies (hydrology, ice load, atmosphere loads, etc).
We included a statement on this in the conclusions (see earlier).

Last paragraph: I am not sure whether this should be part of the conclusion. It may be sufficient to say that Elmer/Earth performs well in parallel computation.

As this is a technical paper that also should inform the reader on the applicability – including computational aspects – of the new code, we believe that this paragraph has a place in the conclusions.

New References

R. Greve, Glacial Isostasy: *Models for the Response of the Earth to Varying Ice Loads*, in B. Straughan, R. Greve, H. Ehrentraut, and Y. Wang (edt.), Continuum Mechanics and Applications in Geophysics and the Environment, Springer, Berlin, Germany etc., 393 pp. (2001). ISBN: 3-540-41660-9

R. Greve and H. Blatter, *Dynamics of Ice Sheets and Glaciers*, Springer, Berlin, Germany (2009) DOI 10.1007/978-3-642-03415-2

Wu, P. & Johnston, P., 1998. *Validity of Using Flat-Earth Finite Element Models in the Study of Postglacial Rebound*. in Dynamics of the Ice Age Earth, pp. 191-202, ed. Wu, P. Trans Tech Publications Ltd, Switzerland.

Schoof, C., 2007. *Ice sheet grounding line dynamics: Steady states, stability, and hysteresis*, Journal of Geophysical Research: Earth Surface, 112, F03S28.

A new open-source ~~visco-elastic~~ viscoelastic solid Earth deformation module implemented in Elmer (v8.4)

Thomas Zwinger[1], Grace A. Nield[2,3], Juha Ruokolainen[1], and Matt A. King[2]

[1]CSC–IT Center for Science Ltd., Espoo, Finland
[2]Surveying and Spatial Sciences, School of Technology, Environments and Design, University of Tasmania, Australia
[3]Department of Geography, Durham University, Durham, UK

Correspondence: Thomas Zwinger (zwinger@csc.fi)

Abstract. We present a new, open source ~~visco-elastic~~ viscoelastic solid Earth-deformation model, Elmer/Earth. Using the multi-physics ~~Finite Element~~ finite element package Elmer, a model to compute ~~visco-elastic~~ viscoelastic material deformation has been implemented into the existing linear elasticity solver routine. Unlike approaches often implemented in engineering codes, our solver accounts for the restoring force of buoyancy within a system of layers with depth-varying density. It does this by directly integrating the solution of the system rather than by applying stress-jump conditions in the form of Winkler foundations on inter-layer boundaries, as is usually needed when solving the minimisation problem given by the stress-divergence in commercial codes. We benchmarked the new model with results from a commercial ~~Finite Element~~ finite element engineering package (ABAQUS, v2018) and another open-source code that uses ~~visco-elastic~~ viscoelastic Normal Mode theory, TABOO, using a flat-earth setup loaded by a cylindrical disc of 100 km diameter and 100 m height of ice density. Evaluating the differences of predicted surface deformation at the centre of the load and two distinctive distances (100 km and 200 km), average deviations of 7 cm and 2.7 cm of Elmer/Earth results to ABAQUS and TABOO, respectively, were observed. In view of more than 100 cm maximum vertical deformation and the different numerical methods and parameters, these are very encouraging results. Elmer is set up as a highly scalable parallel code and distributed under the (L)GPL license, meaning that large scale computations can be made without any licensing restrictions. Scaling figures presented in this paper show good parallel performance of the new model. Additionally, the high fidelity ice sheet code Elmer/Ice utilises the same source-base of Elmer and thereby the new model opens the way to undertaking high-resolution coupled ice-flow - solid Earth deformation simulations, which are required for robust projections of future sea-level rise and glacial isostatic adjustment.

1 Introduction

Reconstructing ice sheet history and predicting ice sheet response to changes in climate is imperative for accurately predicting future ice-mass loss and hence sea-level rise. An important component of ice-sheet evolution is the isostatic response of the solid earth that occurs as a result of changes in the mass of the ice sheet. Over glacial cycles the waxing and waning of ice sheets causes the underlying earth to deform as the ice loading at the surface grows and shrinks. This deformation occurs both instantaneously as an elastic response and over longer timescales as the viscous mantle flows back to previously glaciated regions in order to regain gravitational equilibrium. How fast or slow the earth deforms depends on the underlying mantle

viscosity, and, although typically thought to occur over several thousands of years (Whitehouse, 2018, and references therein), recent studies have ~~showed~~ shown regions undergoing much more rapid (decadal) rebound in response to present-day changes (Nield et al., 2014; Barletta et al., 2018).

This isostatic response of the bedrock can strongly influence ice-sheet dynamics. Deformation of the earth changes the elevation of the ice sheet which in turn affects the surface temperature and the rate of accumulation or ablation. Solid earth deformation also alters the gradient of the bedrock on which the ice sheet rests, particularly at the periphery, altering the internal forces as well as the driving stress and therefore the flow of the ice sheet ~~(Le Meur and Huybrechts, 1996)~~ (Le Meur and Huybrechts, 1996; Adhikari et al., 2014) . In marine-grounded ice sheets lying on a reverse slope bed (e.g. West Antarctica) these effects can be critical. As the grounding line retreats further along the reverse slope into deeper water, ice flux across the grounding line increases leading to increased loss (Schoof, 2007). However, bedrock uplift can have a stabilising effect by reducing the slope of the reverse bed and thereby slowing the retreat of the grounding line (Gomez et al., 2010, 2013).

Including the isostatic response of bedrock in an ice-sheet model is therefore crucial to obtaining accurate predictions of ice-sheet mass balance, and there are several methods which can be used. Computing the isostatic response with a self-gravitating ~~visco-elastic~~ viscoelastic spherical earth is the most accurate, but most computationally expensive, method. Several simple approximations are often made using models with a combinations of local lithosphere or elastic lithosphere with diffusive asthenosphere or relaxing asthenosphere (Le Meur and Huybrechts, 1996; Rutt et al., 2009). Of these, Le Meur and Huybrechts (1996) found the best performing is the "ELRA" (e.g., Greve, 2001) model (elastic lithosphere with relaxing asthenosphere) ~~and~~ which is widely used in ice-sheet modelling , mainly due to its simplicity and fast computations. However, Bueler et al. (2007) found significant differences in resulting bed elevation and ~~ice sheet~~ ice-sheet thickness when using a model with ELRA compared to a spherical self-gravitating model due to the shortcomings of using a constant relaxation time for the mantle as opposed to mode-dependent relaxations times (Peltier, 1974).

A further improvement to an ice-sheet model can be made by coupling a model of solid earth deformation to the ice-sheet model. Studies have demonstrated that the feedback between the two systems can have large impacts on ice sheet evolution (Gomez et al., 2013; de Boer et al., 2014). Using a coupled model Gomez et al. (2015) showed a reduced estimate of Antarctic ice-mass loss compared with a model without solid earth effects included. However, due to the large computational expense of these models, they remain at a relatively low resolution both spatially and temporally therefore omitting short wavelength and short timescale deformations. A recent study by Larour et al. (2019) showed that models need kilometre-scale resolution in the horizontal components to accurately predict ice-sheet evolution in the region of ice sheet mass change, particularly for the short wavelength elastic component of solid earth deformation. This demonstrates the clear need for a full Stokes ice-sheet model capable of computing high resolution solid Earth rebound.

Wu (2004) presented a recipe to adapt existing commercial ~~Finite Element~~ finite element codes to compute earth deformation as a response to ice loads, both for flat-earth as well as spherical self-gravitating setups. Finite ~~Elements~~ elements have the advantage that they in general can use unstructured meshes in order to ~~resolve regions with expected high gradients~~ provide the needed resolution in regions where either physics or geometry demand it while keeping the model size limited. Many

~~Finite Element~~ finite element packages also include versatile solution methods that often also work in parallel computing environments – an essential feature to address continental-size problems at high resolution.

2 Mathematical and numerical model

The implementation of the ~~visco-elastic~~ viscoelastic rheology and additional force terms to a large extent follows the one suggested by Wu (2004). Adopting their notation, we start from the ~~visco-elastic~~ viscoelastic stress tensor, $\boldsymbol{\tau}$ defined by the differential equation

$$\frac{\partial \boldsymbol{\tau}}{\partial t} = \frac{\partial \boldsymbol{\tau}_0}{\partial t} + \frac{\mu}{\nu}\left(\boldsymbol{\tau} - \Pi \mathbf{1}\right), \tag{1}$$

with the stress $\boldsymbol{\tau}_0$ in case of incompressibility given by

$$\boldsymbol{\tau}_0 = \Pi \mathbf{1} + 2\mu\boldsymbol{\epsilon}, \tag{2}$$

where Π denotes the isotropic part of the Cauchy stress, i.e., the pressure. In the derivatives of (1) and (2), t stands for time, $\mathbf{1}$ denotes the unit-tensor, μ the shear modulus and ν is the viscosity. The strain-tensor $\boldsymbol{\epsilon}$ written in terms of the ~~deformation vector~~ displacement $\boldsymbol{d}$ denotes as

$$\boldsymbol{\epsilon} = \mathrm{sym}(\nabla \boldsymbol{d}) = \frac{1}{2}\left(\nabla \boldsymbol{d} + (\nabla \boldsymbol{d})^{\mathrm{T}}\right). \tag{3}$$

The linearised equation of motion ~~(conservation of linear momentum)for a non-selfgravitating~~ for solid earth deformation (Wu, 2004) is given by

$$\nabla \cdot \boldsymbol{\tau} - \nabla(\rho_0 \boldsymbol{g}_0 \dot{d}) - \rho_1 \boldsymbol{g}_0 - \boldsymbol{g}_0 \nabla \phi_1 = \mathbf{0}. \tag{4}$$

Where ρ_0 and $\boldsymbol{g}_0$ are hydrostatic background density and gravity, respectively, and ρ_1 is the perturbed density. The direction of $\boldsymbol{g}_0$ is in negative radial direction. According to Wu (2004, section 3) ~~(2004~~, a flat-earth model is derived from (4) by assuming incompressibility and ignoring self-gravitational effects (i.e., redistribution of mass), making the third and fourth terms vanish. Further, sphericity is ignored, leading to changes aligned with the unit vector of a Cartesian system in vertical direction, $\boldsymbol{e}_z$. This leads to the equation of motion for a non-self-gravitating flat-earth model with layer-wise constant material~~is expressed in terms of~~. It reduces to a balance between the divergence of the stress (first term) and a restoring force due to the advection of pre-stress of the material (Wu, 2004)

$$\nabla \cdot \boldsymbol{\tau} - \rho g \nabla(\boldsymbol{e}_z \cdot \boldsymbol{d}) = \mathbf{0}. \tag{5}$$

Here, ~~$g = ||\boldsymbol{g}||$~~ $\rho = \rho_0$ and $g = ||\boldsymbol{g}_0||$ is the magnitude of the local acceleration by gravity, which points into the negative direction of $\boldsymbol{e}_z$. ~~Consequently, the inner vector-product $d_z = \boldsymbol{e}_z \cdot \boldsymbol{d}$ is the deformation aligned with the axis of gravity.~~

2.1 Implementation in Elmer/Earth

Elmer/Earth is based on the open-source ~~Finite Element~~ finite element package Elmer (Råback et al., 2019). In order to build a ~~flat-Earth~~ flat-earth model as described in the previous section, equation (1) has been added to the already existing linear elasticity solver of Elmer. In case of incompressibility, the additional variable of pressure, Π , has been introduced to the solver. This avoids the singularity of the compressible formulation in the case of the Poisson ratio approaching $1/2$.

Many commercial codes lack an implementation of the second term in (5), which implies a transformation of the stress to reduce the formulation to only the first term. As a consequence of this stress transformation, additional jump-conditions in the form of Winkler foundations (Wu, 2004) have to be imposed on internal boundaries that mark a jump in either the gravity or the density. This can be inconvenient in building the model, as a detailed description of the setup may contain boundaries for more than 10 layers.

Here we take advantage of the accessibility of the source code of Elmer by including this term in the weak formulation that uses the ~~visco-elastic~~ viscoelastic stress. The second term in (5) thereby contributes to the stiffness matrix. Naturally, the formulation still needs a layered structure of the model, i.e., material parameters are kept constant for certain layers. This can be easily achieved as Elmer allows material parameters to be prescribed as well as body forces (in our case gravity), on the basis of elements or even integration-points (in addition to nodal values). This means that we are able to impose discontinuities in parameters over elements anywhere in the discretized computing domain without placing Winkler foundation boundaries at layer interfaces. In other words, no boundary conditions have to be set at internal layer boundaries. By including this term in the weak formulation of the problem, the method then automatically applies the needed restoring force on element boundaries with jumps in material properties or gravity, without the need to place boundaries in the mesh.

Discretization of the time derivatives for stress and pressure (in case of incompressible material) is implemented by the first-order implicit difference,

$$\frac{\partial \boldsymbol{\tau}}{\partial t} \approx \frac{\boldsymbol{\tau}^{\mathrm{i}+1} - \boldsymbol{\tau}^{\mathrm{i}}}{\Delta t}, \quad \frac{\partial \Pi}{\partial t} \approx \frac{\Pi^{\mathrm{i}+1} - \Pi^{\mathrm{i}}}{\Delta t}. \tag{6}$$

Here, i is the current, and $\mathrm{i}+1$ the implicit time-step as well as $\Delta t = t^{\mathrm{i}+1} - t^{\mathrm{i}}$ the time-step size between. The solution of the time-evolution problem reads then as

$$-\mathbf{1}\Pi^{\mathrm{i}+1} + 2\,\mu\Phi\boldsymbol{\epsilon}^{\mathrm{i}+1} = -\Phi\Pi^{\mathrm{i}} + 2\,\mu\Phi\boldsymbol{\epsilon}^{\mathrm{i}} - \Phi\boldsymbol{\tau}^{\mathrm{i}}, \tag{7}$$

with $\phi = 1/(1 + (\mu/\nu)\Delta t)$. The balance (5) of linear momentum is then solved for the new ~~timestep~~ time step

$$\nabla \cdot \boldsymbol{\tau}^{\mathrm{i}+1}(\boldsymbol{d}) - \rho g \nabla \left(\boldsymbol{e}_z \cdot \boldsymbol{d}^{\mathbf{i+1}}\right) = \mathbf{0}. \tag{8}$$

The weak formulation then results from the integral over the whole domain Ω (with its confining surface $\partial\Omega$) using the test and weighting function vectors $\boldsymbol{u}, \boldsymbol{v} \in H^1$

$$\int_\Omega \tau(\boldsymbol{u}) \cdot (\nabla \boldsymbol{v})\, dV - \oint_{\partial\Omega} (\tau(\boldsymbol{u}) \cdot \boldsymbol{n}) \cdot \boldsymbol{v}\, dA - \int_\Omega \rho g \nabla (\boldsymbol{e}_z \cdot \boldsymbol{u}) \cdot \boldsymbol{v}\, dV = 0. \tag{9}$$

Mind that the divergence of the stress tensor has been partially integrated, leading – after Green's theorem – to a term that integrates the stress vector, $\boldsymbol{t} = \tau(\boldsymbol{u}) \cdot \boldsymbol{n}$ over $\partial\Omega$ with its surface normal $\boldsymbol{n}$. Taking additionally into account that $\tau(\boldsymbol{u})$ is a symmetric tensor, only the symmetric part of $\mathrm{sym}(\nabla \boldsymbol{v}) = \boldsymbol{\epsilon}(\boldsymbol{v})$ contributes to the first integral, leading to the symmetric stiffness matrix in the weak formulation

$$\int_\Omega \tau(\boldsymbol{u}) \cdot \boldsymbol{\epsilon}(\boldsymbol{v})\, dV - \oint_{\partial\Omega} (\tau(\boldsymbol{u}) \cdot \boldsymbol{n}) \cdot \boldsymbol{v}\, dA - \int_\Omega \rho g \nabla (\boldsymbol{e}_z \cdot \boldsymbol{u}) \cdot \boldsymbol{v}\, dV = 0. \tag{10}$$

The system is completed by boundary conditions that are either provided by a value for any component of the stress-vector, $\boldsymbol{t} = \boldsymbol{\tau} \cdot \boldsymbol{n}$, in the second integral (Neumann condition) of equation (10) or by imposing a value for any component of the deformation vector, $\boldsymbol{d}$ (Dirichlet condition).

Equation (10) is solved using the standard Galerkin method with – in the case of the benchmark described in section 3 – first order basis functions. Apart from this particular choice, Elmer provides a variety of possible basis functions left to the choice of the user. The iteration for the viscous contribution is computed on the Gaussian integration points. In case of incompressibility, stabilization has to be applied by the residual free bubble method.

3 Benchmark tests

Benchmark tests are performed in order to validate the new implementation of Elmer/Earth in comparison to two other codes, ABAQUS and TABOO. We force the models with changing surface load, representing an idealised ice loading experiment. Specific geometry, earth structure and ice loading for the benchmarking case are described in Section 3.3. The two other codes are briefly introduced in the following sections.

3.1 Reference model ABAQUS

We use the finite element software package ABAQUS (Hibbitt et al., 2016, software version 2018) to construct a model to verify the results of the new ~~visco-elastic~~ viscoelastic solver implemented in Elmer. We choose this approach to replicate as fully as possible the geometry and equations implemented in the Elmer/Earth model. The model is a 3-D flat-earth model which computes the solid Earth deformation in response to a changing surface load using the approach of (Wu, 2004). Buoyancy forces are accounted for by applying Winkler foundations to layer boundaries within the model where a density contrast occurs between two layers, and at the surface (Wu, 2004). The model has a large lateral extent to prevent boundary effects in the area of interest (Steffen et al., 2006) and ~~the model is fixed in all directions at the sides and the base~~has zero displacement imposed on its lateral and bottom boundaries. The model includes layers from the surface of the Earth to the core-mantle boundary with parameters shown in Table 1.

3.2 Reference model TABOO

TABOO is an open source post-glacial rebound calculator (Spada et al., 2003; Spada, 2003) that computes the deformation of the Earth in response to a changing surface (glacial) load. The TABOO model assumes a spherically symmetric, incompressible

earth with a Maxwell ~~visco-elastic~~ viscoelastic rheology (non-rotating, self-gravitational). TABOO implements the classical ~~visco-elastic~~ viscoelastic normal mode method commonly used in studies of glacial isostatic adjustment (Peltier, 1974). There are several inbuilt solid Earth models available in TABOO with specific earth structure and parameters and we use one of these for our synthetic benchmarking case study (Table 1, Section 3.3). Deformation is computed up to a user-specified spherical harmonic degree, and we chose 2048 (equivalent to approximately 10km).

3.3 Test model setup

In order to test and compare the newly built Elmer/Earth model, a simple benchmark case has been set up for each of the models presented in Sections 3.1 and 3.2. The benchmark case consists of a simple one-dimensional earth structure with parameters varying in the radial direction only, loaded and unloaded with a disc of ice. The models in Elmer/Earth and ABAQUS both use a flat-earth approximation whereas TABOO is a fully spherical model. The effects of sphericity are negligible for the size of load we use for our benchmarking case. None of the models solve the "sea-level equation" (Farrell and Clark, 1976).

For the flat-earth approximation, the three-dimensional model domain stretches 4000 km in each horizontal direction from the centre of the ice load. This distance is 80 times the diameter of the test load which is more than sufficient to allow mantle deformation below the ice load (Steffen et al., 2006). With depth, the model extends from the Earth's surface at a radius of 6371 km to the core-mantle boundary with a total depth of 2891 km.

Geometry construction and meshing for Elmer/~~Ice~~ Earth simulations was achieved using the open source software Gmsh (Geuzaine and Remacle, 2009). The lateral mesh resolution for ABAQUS model is constant 10 km, whereas it varies for Elmer/Earth from 10 km for the area over which the load is applied, increasing linearly to 200 km at the lateral domain boundaries (see left panel of Fig. ~~??). Top view of the reference run Elmer/Earth mesh (mesh2). Annotated coordinates are in metres~~1). The vertical resolution increases with depth as shown in the right panel of Fig. ~~??~~1. The TABOO model has a spectral resolution equivalent to 10 km.

The earth structure used for the benchmarking case is one that is included as part of the TABOO package and is summarised in Table 1. The solid Earth model consists of an elastic lithosphere, a ~~visco-elastic~~ viscoelastic upper mantle divided into three layers, and a ~~visco-elastic~~ viscoelastic lower mantle. Elmer/Earth applies incompressibility throughout the whole column and an extremely high viscosity of $\nu = 1 \times 10^{44}$ $\mathrm{Pa\,s}$ in the Lithosphere, thereby enforcing an approximately elastic behaviour ~~.~~ on the timescale of the load. This can be justified by the Maxwell-time $t_M = \nu/\mu$ being of the order of 10^{33}s, which indicates that viscous effects only would be significant at timescales several order of magnitudes larger than the timing of the load signal.

The viscosity of the upper and lower mantle is set to 1×10^{18} and 1×10^{22} $\mathrm{Pa\,s}$, respectively, and the elastic and density parameters are depth-averaged values from the Preliminary Reference Earth Model (Dziewonski and Anderson, 1981, PREM). These parameters can easily be assigned to layers in both ABAQUS and Elmer. The relatively low value for the upper mantle helps to shorten the timescales for the benchmark test.

For the benchmark case we compute the deformation caused by an instantaneously imposed ice load at ~~zero time~~$t = 0$. Starting from an equilibrium bedrock with zero deformation, an ice load is instantaneously applied at the centre of the domain at the very beginning of the simulation. It is a 100 km diameter disc of 100 m height with a prescribed constant density of

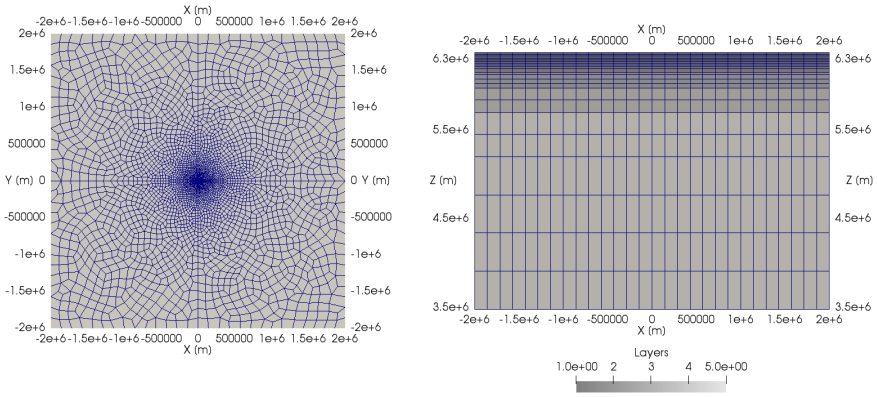

Figure 1. ~~Side~~ Top and side view of the reference run Elmer/Earth mesh (~~mesh2~~mesh1)~~showing the~~ . The different layers corresponding to varying material parameters shown in the right panel are given in Tab, 1. Annotated coordinates are in metres

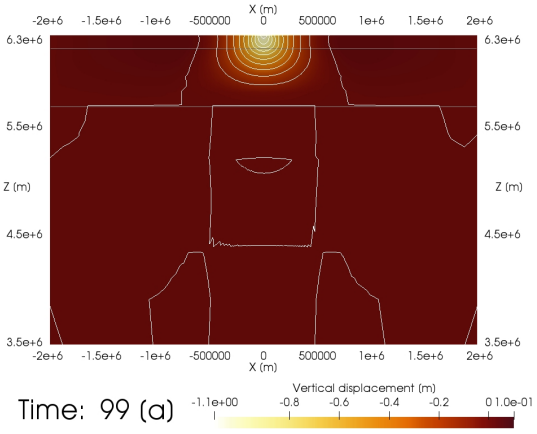

Figure 2. Cross section of the reference run with Elmer/Earth (mesh1) showing the vertical deformation at 99 years into the simulation at maximum deformation. Deformation is shown as colour texture as well as iso-line (white in 0.1 m spacing). The boundaries between the lithosphere, upper and lower mantle (as given in Tab, 1) are annotated as black lines . Annotated coordinates are in metres

917 $\mathrm{kg\,m^{-3}}$. The load is maintained for 100 years after which it is instantaneously removed and the rebound computed for a further 100 years. The result on the vertical plane of symmetry from the reference run described in Sect. 5 is shown in Fig. 2. The temporal evolution of the vertical displacement of the reference Elmer/Earth run (mesh1) over a line at the surface from centre to the margin (0-200 km) is depicted in Fig.3.

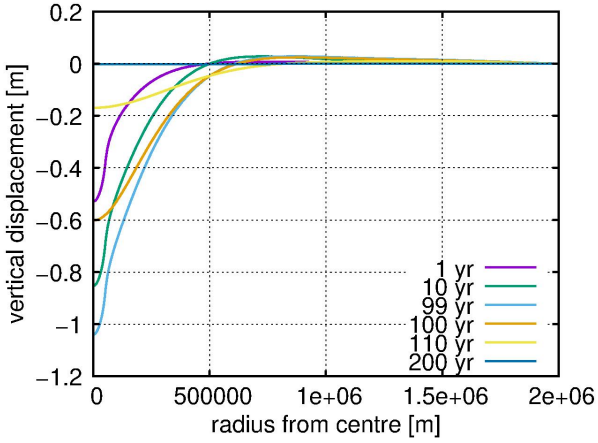

Figure 3. Temporal evolution of vertical displacement of the reference Elmer/Earth run (`mesh1`) over a line at the surface from centre to the margin

Table 1. Properties of the different layers in the flat-Earth model benchmark. Vertical distances are with respect to Earth's centre. The ABAQUS reference model uses ~~compressible~~ a material model with a constant Poisson's ratio of 0.49 throughout the whole domain.

Layer	vertical range [km]	thickness [km]	ϱ [kg m^{-3}]	g [m s^{-2}]	ν[Pa s]	E [Pa]
Lithosphere:	6371-6251	120	3233	9.87852	0 or 1×10^{44}	1.8388×10^{11}
Upper mantle:	6251-6151	100	3367.12	9.939356456	1×10^{18}	1.9941×10^{11}
	6151-5971	180	3475.58	9.875562964	1×10^{18}	2.2948×10^{11}
	5971-5701	270	3857.75	9.839990347	1×10^{18}	3.1943×10^{11}
Lower mantle:	5701-3480	2221	4877.91	9.792107051	1×10^{22}	6.5844×10^{11}

3.4 Numerical settings in Elmer/Earth

For all runs of Elmer/Earth presented in sections 4 and 5, the same numerical methods and parameters have been applied. A time-step size for the implicit backward differentiation formula (BDF) of the equivalent of one year has been chosen – in Section 5 we discuss the impact in accuracy by halving this time-step size. The resulting system matrix of the linear elasticity solver was first pre-conditioned using an ILU (Incomplete Lower-Upper) factorisation of first order degree (ILU1, in Elmer terminology). To obtain a solution, its inverse was approximated using the GCR (Generalized Conjugate Residual) Krylov-subspace method ~~(Eisenstat et al., 1983; Barrett et al., 1993, see e.g.)~~(see e.g. Eisenstat et al., 1983; Barrett et al., 1993). A convergence criterion was applied for the relative norm of the solution vector between two iteration steps of $\varepsilon_{\boldsymbol{d}} = 1 \times 10^{-7}$.

4 Comparison of results

Comparing the results of the benchmarking exercise with two models that use different methods gives us confidence in the implementation of the new Elmer code. Figure 4 shows displacement with time at three locations - the centre of the disc (indicated by 0 km) and at 100 km and 200 km distance from the centre of the disc. The displacement curves for all three

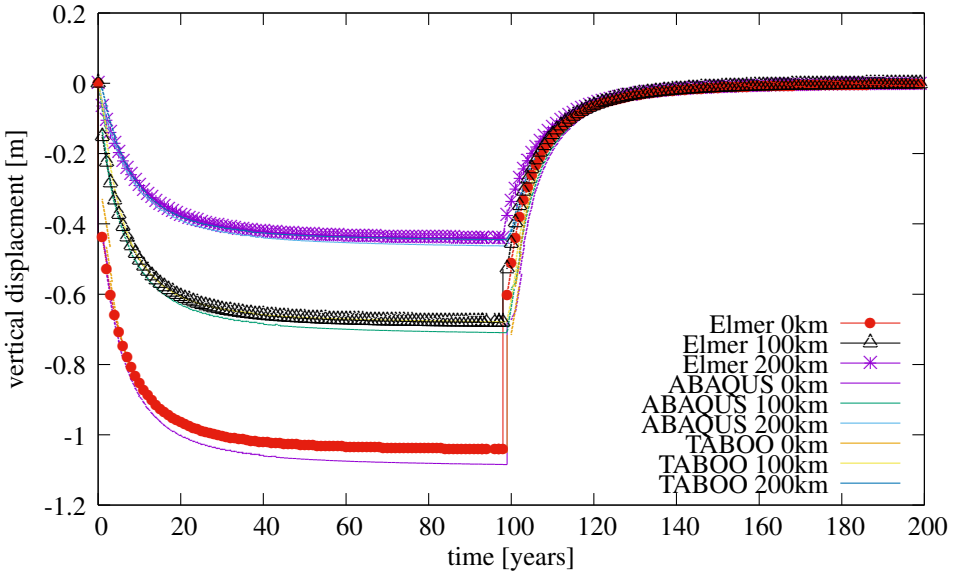

Figure 4. Comparison of results for deformation at load-centre (0 km), 100 and 200 km for Elmer/Earth, ABAQUS and TABOO.

models over major parts of the simulation agree to within an order of 10 cm (see Fig. 5) in relation to a maximum deformation of 1.1 m by ABAQUS at the centre. The largest difference is observed at the centre of the disc where the Elmer/Earth model deforms slightly less than ABAQUS and almost insignificantly more as TABOO, but reaches this deformation more quickly than the other codes (i.e. has a faster relaxation time). As a consequence, Fig. 5 shows differences in vertical displacement between models (also between ABAQUS and Taboo) to be largest in the very beginning, when applying the load) and around the time of sudden deloading.

The small differences between the results could be caused by several factors. Mesh differences between Elmer/Earth and ABAQUS are the likely cause of some small differences with ABAQUS having a regular grid mesh and Elmer having a finer mesh at the centre of the disc. There seems to be a correlation of the resolution in the centre with the displacement in both FEM based models. It seems that the ABAQUS model setup does not provide enough horizontal mesh resolution at the centre, where the load is applied. This is confirmed by results obtained with `mesh 2` (half mesh size) in Elmer/Earth, which produced displacements even larger than the one with the constant 25 km mesh from ABAQUS (see Section 5).

The deformation calculated by TABOO is less than Elmer/Earth and ABAQUS at each location. This may be due to the fundamental differences in the computation methods employed by the TABOO code, implementing normal mode methods rather

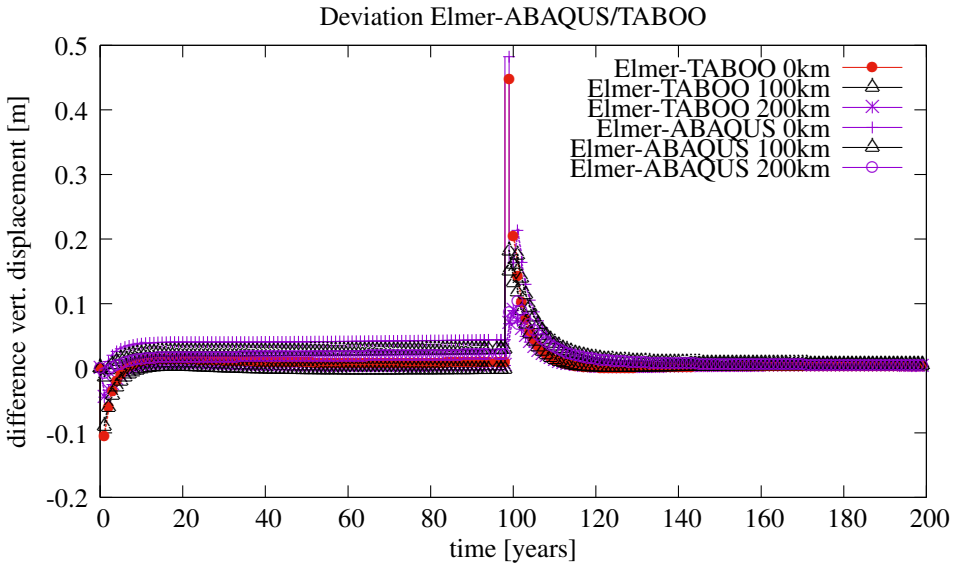

Figure 5. Difference of deformation at load-centre (0 km), 100 and 200 km of Elmer/Earth relative to ABAQUS and TABOO.

Table 2. Parameters of the meshes and their partitions used for Elmer/Earth test runs

Mesh name	no. nodes	no. elements	no. partitions
`mesh1` (reference)	87745	82676	16 and 32
`mesh2` (half size)	44198	41328	16 and 32
`mesh3` (double size)	160747	152152	64

than finite element methods. Furthermore, TABOO computes deformation on a self-gravitating solid Earth whereas ABAQUS and Elmer do not include self-gravitation, which would result in some differences between these models. Nevertheless, the differences observed in the displacement curves are still within an acceptable tolerance.

5 Performance and accuracy of the Elmer/Earth deformation model

In order to obtain some insight into parallel performance as well as the dependency on mesh resolution of Elmer/Earth, three meshes with different resolutions and mesh partitions (4, 16 and 32) have been created (see Table 2). Partitioning of the meshes has been performed by the mesh-conversion program `ElmerGrid` (part of the Elmer installation) using the METIS k-way partitioning scheme (Karypis and Kumar, 1998). Identical numerical parameters and methods, as described in Sect. 2, were applied throughout all runs.

Table 3. Timings of different scalability test runs. All timings are given in seconds

Mesh (case)	partitions	CPU time [s]	wall-clock time [s]
`mesh1` (single node)	16	19702	21288
`mesh1` (reference)	32	9016	9639
`mesh1` (half time-step size)	32	14319	16351
`mesh2` (half size, 1 node)	16	5035	6122
`mesh2` (half size, 2 nodes)	32	3271	3683
`mesh3` (double size)	64	14817	15800

5.1 Strong and weak scaling

Tests were performed on the Linux cluster `raijin` (Australian National Computational Infrastructure, 2017), utilising compute nodes, each equipped with two Intel Xeon Sandy Bridge (E5-2670, 2.6 GHz) processors summing up to 16 cores per compute node. The code was compiled using the Intel compiler suite (version 2019.2.187) with Open MP (OMP) enabled, mainly to activate utilisation of OMP-SIMD instructions within the code (Byckling et al., 2017). CPU specific optimisation was enabled by compiler flags `-O2 -march=sandybridge`. Basic linear algebra libraries (Lapack, BLAS, ScaLapack) were linked in from the Intel MKL library. Message passing was enabled by linking to the Intel MPI library (version 5.1.0.097) provided on the system.

We want to emphasise that we only studied a limited set of problem sizes/computing resource configurations and only single runs (no statistics) were performed. Results presented in the following thus have to be interpreted in view of the limitations. All runs performed are summarised in Table 3.

A comparison of a simulation performed with 16 cores (single compute node) with `mesh2` (half size) and with 32 cores (two compute nodes) on `mesh1` (reference) reveals a drop to 64% of an ideal, linear weak scaling (increasing core numbers while maintaining the load/core) performance. This can be explained by adding additional latency to that part of the MPI communication that in the 32 core run has to be routed over the inter-nodal connection (Infiniband), whereas the 16 core run solely uses faster communication provided within a single compute node. Reassuringly, a similar value, namely 61%, was obtained between runs on the double-size mesh (`mesh3`) with 64 cores on 4 compute nodes in relation to the reference problem (`mesh1`) run on 32 cores on 2 compute nodes. Studying the log-files of the runs, it also comes clear that the chosen GCR algorithm takes longer to converge with respect to the same convergence criteria if increasing the amount of mesh-partitions. Another comparison with slightly less strict convergence criteria of the linear solution iteration algorithm led to a value of 84%.

On the other hand, if looking at strong scalability (i.e., increasing core numbers while reducing load/core), doubling computational resources from 16 cores (single compute node) to 32 cores (inter-nodal) for the fixed-size smaller problem (`mesh2`)

revealed a speedup of 1.66, which is below the ideal value of 2 (half wall-clock time by doubling of cores). For the larger reference problem (`mesh1`), we achieve a speedup of 2.2 if increasing from 16 (single node) to a 32 core utilising two compute nodes of the reference run. We have not further investigated the particular cause of this super-linear scaling, but can speculate on it: ~~Halfing~~ Reducing the needed memory/core improves the possibility to fit more data into the cache and thereby enable faster memory access (i.e., avoiding cache misses) and hence – despite the added latency from inter-nodal communication– allowing for a general acceleration.

Despite applying the same solution method, it is not really possible to compare performance of Elmer/Earth to ABAQUS, since the latter was run on a different platform using a regular mesh of 25 km constant horizontal mesh size. Computational performance was not the main motivation behind using ABAQUS for the benchmarking exercise, rather we wanted to use a model that could best replicate the geometry and equations used. Nevertheless, it is interesting to note that the run-time of ABAQUS was in the range of 6 h using 32 cores on an high-end workstation, hence about twice the time of Elmer/Earth reference run on the same amount of cores of a larger Linux cluster. These run-times should not be used in a direct comparison for computational performance, since ABAQUS was run on a mesh significantly larger (600k nodes) than the one of Elmer/Earth. However, TABOO is using a completely different model approach, such that any comparison would be obsolete.

5.2 Accuracy with respect to mesh and time-step size

We further studied accuracy and consistency of Elmer/Earth results with respect to spatial and temporal discretization sizes. To that end, we ran the same numerical setup on all three meshes given in Tab. 2. Results are depicted in Fig. 6 and reveal

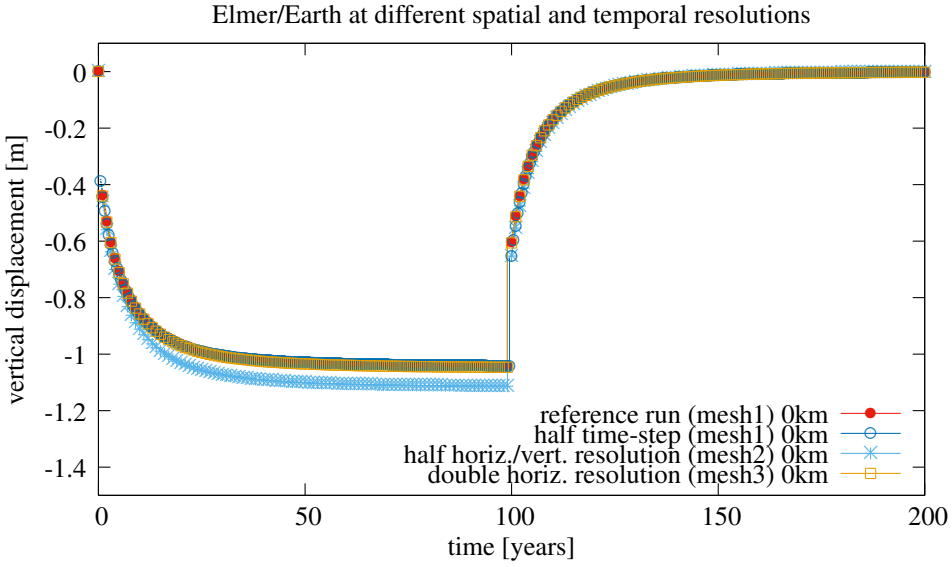

Figure 6. Vertical deformation at the centre (0 km) of Elmer/Earth simulations using different spatial and temporal resolutions.

that too low spatial resolution (i.e., `mesh2`) – in that particular case in horizontal as well as vertical direction – yields too

large deformations. That might simply be because of too little resolution of the induced viscous deformation in under-resolved layers. The finer resolved meshes (`mesh1` and `mesh3`) show very little deviations in results, thus indicating consistency of the model beyond a resolution of about 5 km mesh-size at the centre of the geometry and the vertical structure depicted in the right panel of Fig. ??1. On the other hand, increasing temporal accuracy by reducing the time-step size from one year to half a year did not reveal any significant difference in result for similar setups to the reference run (`mesh1`).

6 Conclusions

We presented a newly implemented ~~visco-elastic~~ viscoelastic addition to the linear elasticity solver of the open-source ~~Finite Element~~ finite element package Elmer and its application to a flat-earth model. Robust projection of future ice sheet change depends on coupled solid Earth and ice dynamic processes at high spatial resolution, and Elmer/Earth provides a new open source capability in conjunction with the existing ice-sheet model Elmer/Ice (Gagliardini et al., 2013). Elmer/Earth, on its own, provides a new tool for modelling ~~visco-elastic~~ viscoelastic solid Earth deformation due to surface loading changes.

Elmer/Earth for the time being is a so-called flat-earth model (Wu, 2004). In its current state it ignores sphericity and self-gravitational effects as well as neglects to account for the deformation induced by redistribution of ocean water masses. This introduces certain limitations on its applicability (Wu and Johnston, 1998). Consequently, future applications of this particular model version should be confined to regional studies of ice-sheets or highly localised loads, such as glaciers and ice-caps.

We benchmarked Elmer/Earth with another FEM code, ABAQUS, as well as a spherical ~~visco-elastic~~ viscoelastic normal mode code, TABOO, and these comparisons show good agreement in the range of deviation in solution method as well as numerical approaches.

Scaling figures presented in Sect. 5 are what one would expect from other parallel performance tests of Elmer. A good performance tuning strategy will have to make sure that a good ratio between partition size (i.e., computation mainly bounded by memory access) and communication between the different MPI tasks is obtained. OpenMP multi-threading in principle is available for certain modules in Elmer, yet, not implemented for the linear elasticity solver, but might give some potential to boost performance within a single node (Byckling et al., 2017).

Code availability. Elmer (version 8.4) is available for download under GitHub. The revision (SHA-1 14c19b6) used in this study can be retrieved from https://github.com/ElmerCSC/elmerfem/archive/14c19b681beb12df3a1d88fed9cd56a694b0cc92.zip (last visited 2019-11-06). TABOO is an open source code available for download under GitHub. In this study we used version v1.1 (SHA-1 6163bec), which can be downloaded from https://github.com/danielemelini/TABOO/archive/v1.1.zip (last visited 2019-11-06). ABAQUS is proprietary software and needs a purchased license. We used ABAQUS 2018 release in this study. Information on how to obtain the software can be found under https://www.3ds.com/products-services/simulia/products/abaqus/ (last visited 2019-11-06).

~~ABAQUS is proprietary software and needs a purchased license. We used ABAQUS 2018 release in this study. Information on how to obtain the software can be found under https://www.3ds.com/products-services/simulia/products/abaqus/ (last visited 2019-11-06).~~

Video supplement. https://doi.org/10.5446/44086

Author contributions. TZ helped developing and implementing the model setup and performing the computations in Elmer. GN contributed to the design of the benchmark setup and performed the computations in ABAQUS and TABOO. JR implemented the altered model equations in the source code of Elmer. MK conceived the study and consulted in the model implementation and contributed to the design of the benchmark test. All authors contributed to the manuscript

Competing interests. None

Acknowledgements. Development of the ~~visco-elastic~~ viscoelastic model was supported under Australian Research Council's Special Research Initiative for Antarctic Gateway Partnership (Project ID SR140300001) and Discovery Project DP170100224. Part of the work of Thomas Zwinger was enabled by a visiting scientist scholarship from UTAS. This research was undertaken with the assistance and resources from the the National ~~Computing~~ Computational Infrastructure (NCI Australia), an NCRIS enabled capability supported by the Australian Government. We want to express our gratitude to Dr. Peter Råback (CSC) for solving a problem with post-processing of Elmer/Earth data and Dr. Fredrik Robertsén (CSC) for the discussion on scalability test results. We are grateful to Giorgio Spada for making TABOO open source.

References

Adhikari, S., Ivins, E. R., Larour, E., Seroussi, H., Morlighem, M., and Nowicki, S.: Future Antarctic bed topography and its implications for ice sheet dynamics, Solid Earth, 5, 569–584, https://doi.org/10.5194/se-5-569-2014, 2014.

Australian National Computational Infrastructure: Online description of `raijin` system, https://nci.org.au/systems-services/peak-system/raijin/, last accessed 2019-07-19, 2017.

Barletta, V., Bevis, M., Smith, B., Wilson, T., Brown, A., Bordoni, A., Willis, M., Khan, S., Rovira-Navarro, M., Dalziel, I., Smalley, R., Kendrick, E., Konfal, S., Caccamise, D., Aster, R., Nyblade, A., and Wiens, D.: Observed rapid bedrock uplift in Amundsen Sea Embayment promotes ice-sheet stability, Science, 360, 1335–1339, https://doi.org/10.1126/science.aao1447, 2018.

Barrett, R., Berry, M., Chan, T. F., Demmel, J., Donato, J., Dongarra, J., Eijkhout, V., Pozo, R., Romine, C., and Van der Vorst, H.: Templates for the Solution of Linear Systems: Building Blocks for Iterative Methods, SIAM, https://doi.org/10.1137/1.9781611971538, 1993.

Bueler, E., Lingle, C., and Brown, J.: Fast computation of a viscoelastic deformable Earth model for ice-sheet simulations, Annals of Glaciology, 46, 97–105, https://doi.org/10.3189/172756407782871567, 2007.

Byckling, M., Kataja, J., Klemm, M., and Zwinger, T.: OpenMP SIMD Vectorization and Threading of the Elmer Finite Element Software, in: Proceedings 13th International Workshop on OpenMP, pp. 123–137, Springer Lecture Notes, https://doi.org/10.1007/978-3-319-65578-9_9, 2017.

de Boer, B., Stocchi, P., and van de Wal, R.: A fully coupled 3-D ice-sheet–sea-level model: algorithm and applications, Geosci. Model Dev., 7, 2141–2156, https://doi.org/10.5194/gmd-7-2141-2014, 2014.

Dziewonski, A. and Anderson, D.: Preliminary reference Earth model, Phys. Earth planet. Inter., 25, 297–356, https://doi.org/10.1016/0031-9201(81)90046-7, 1981.

Eisenstat, S., Elman, H., and Schultz, M.: Variational iterative methods for nonsymmetric systems of linear equations, SIAM J. Numer. Anal., 20, 345–357, 1983.

Farrell, W. and Clark, J.: On Postglacial Sea Level, Geophys. J. Roy. Astr. S., 46, 647– 667, https://doi.org/10.1111/j.1365-246X.1976.tb01252.x, 1976.

Gagliardini, O., Zwinger, T., Gillet-Chaulet, F., Durand, G., Favier, L., Fleurian, B., Greve, R., Malinen, M., Martin, C., Råback, P., Ruokolainen, J., Sacchettini, M., Schäfer, M., Seddik, H., and Thies, J.: Capabilities and performance of Elmer/Ice, a new-generation ice sheet model, Geoscientific Model Development, 6, https://doi.org/10.5194/gmd-6-1299-2013, 2013.

Geuzaine, C. and Remacle, J.-F.: Gmsh: A 3-D finite element mesh generator with built-in pre- and post-processing facilities, International Journal for Numerical Methods in Engineering, 11, 1309–1331, https://doi.org/10.1002/nme.2579, 2009.

Gomez, N., Mitrovica, J., Huybers, P., and Clark, P.: Sea level as a stabilizing factor for marine-ice-sheet grounding lines, Nature Geosci., 3, 850–853, https://doi.org/10.1038/ngeo1012, 2010.

Gomez, N., Pollard, D., and Mitrovica, J.: A 3-D coupled ice sheet – sea level model applied to Antarctica through the last 40 ky, Earth and Planetary Science Letters, 384, 88–99, https://doi.org/10.1016/j.epsl.2013.09.042, 2013.

Gomez, N., Pollard, D., and Holland, D.: Sea-level feedback lowers projections of future Antarctic Ice-Sheet mass loss, Nature Communications, 6, 8798, https://doi.org/10.1038/ncomms9798, 2015.

Greve, R.: Glacial Isostasy: Models for the Response of the Earth to Varying Ice Loads, in: Continuum Mechanics and Applications in Geophysics and the Environment, pp. 307–325, Springer, Berlin, Germany, https://doi.org/10.1007/978-3-662-04439-1_16, 2001.

Hibbitt, D., Karlsson, B., and Sorensen, P.: Getting Started with ABAQUS, Version (6.14), hibbitt, karlsson & sorensen, inc. edn., 2016.

Karypis, G. and Kumar, V.: Multilevel k-way Partitioning Scheme for Irregular Graphs, Journal of Parallel and Distributed Computing, 48, 96–129, https://doi.org/10.1006/jpdc.1997.1404, 1998.

Larour, E., Seroussi, H., Adhikari, S., Ivins, E., Caron, L., Morlighem, M., and Schlegel, N.: Slowdown in Antarctic mass loss from solid Earth and sea-level feedbacks, Science, 364, 7908, https://doi.org/10.1126/science.aav7908, 2019.

Le Meur, E. and Huybrechts, P.: A comparison of different ways of dealing with isostasy: examples from modeling the Antarctic ice sheet during the last glacial cycle, Annals of Glaciology, 23, 309–317, https://doi.org/10.3189/S0260305500013586, 1996.

Nield, G., Barletta, V., Bordoni, A., King, M., Whitehouse, P., Clarke, P., Domack, E., Scambos, T., and Berthier, E.: Rapid bedrock uplift in the Antarctic Peninsula explained by viscoelastic response to recent ice unloading, Earth and Planetary Science Letters, 397, 32–41, https://doi.org/10.1016/j.epsl.2014.04.019, 2014.

Peltier, W.: The impulse response of a Maxwell earth, Rev. Geophys. Space Phys., 12, 649– 669, https://doi.org/10.1029/RG012i004p00649, 1974.

Rutt, I., Hagdorn, M., Hulton, N., and Payne, A.: The Glimmer community ice sheet model, J. Geophys. Res., 114, F02 004, https://doi.org/10.1029/2008JF001015, 2009.

Råback, P., Malinen, M., Ruokolainen, J., Pursula, A., and Zwinger, T.: Elmer Models Manual, http://www.nic.funet.fi/pub/sci/physics/elmer/doc/ElmerModelsManual.pdf, 2019.

Schoof, C.: Ice Sheet Grounding Line Dynamics: Steady States, Stability, and Hysteresis, Journal of Geophysical Research, 112, F03S28, https://doi.org/10.1029/2006JF000664, 2007.

Spada, G.: The theory behind TABOO, 2003.

Spada, G., Antonioli, A., Boschi, L., Brandi, V., Cianetti, S., Galvani, G., Giunchi, C., Perniola, B., Piana Agostinetti, N., Piersanti, A., and Stocchi, P.: TABOO, User Guide, 2003.

Steffen, H., Kaufmann, G., and Wu, P.: Three-dimensional finite-element modeling of the glacial isostatic adjustment in Fennoscandia, Earth planet. Sci. Lett., p. 358–375, https://doi.org/10.1016/j.epsl.2006.08.003, 2006.

Whitehouse, P.: Glacial isostatic adjustment modelling: historical perspectives, recent advances, and future directions, Earth Surf. Dynam., 6, 401–429, https://doi.org/10.5194/esurf-6-401-2018, 2018.

Wu, P.: Using commercial finite element packages for the study of earth deformations, sea levels and the state of stress, Geophys. J. Int., 158, 401–408, https://doi.org/10.1111/j.1365-246X.2004.02338.x, 2004.

Wu, P. and Johnston, P.: Validity of Using Flat-Earth Finite Element Models in the Study of Postglacial Rebound, in: Dynamics of the Ice Age Earth, pp. 191–202, Trans Tech Publications Ltd, Switzerland, 1998.